sciendo

Int. J. of Applied Mechanics and Engineering, 2018, vol.23, No.3, pp.803-811
DOI: 10.2478/ijame-2018-0044

Brief note

APPLICATION OF THE RIGID FINITE ELEMENT METHOD TO STATIC ANALYSIS OF LATTICE-BOOM CRANES

I. ADAMIEC-WÓJCIK*, Ł. DRĄG and S. WOJCIECH
Division of Computer Modelling, Faculty of Management and Transport
University of Bielsko-Biała, POLAND
E-mails: i.adamiec@ath.bielsko.pl; ldrag@ath.bielsko.pl; swojciech@ath.bielsko.pl

M. METELSKI
Protea sp z o.o.
Galaktyczna 30a, 80-299 Gdansk, POLAND
E-mail: marek.metelski@protea.pl

In the paper a nonlinear model of a lattice-boom crane with lifting capacity up to 700mT for static analysis is presented. The rigid finite element method is used for discretisation of the lattice-boom and the mast. Flexibility of rope systems for vertical movement and for lifting a load is also taken into account. The computer programme developed enables forces and stress as well as displacements of the boom to be calculated. The model is validated by comparison of the authors' own results with those obtained using professional ROBOT software. Good compatibility of results has been obtained.

Key words: rigid finite element method, static analysis, lattice-boom crane, flexibility of rope systems

1. Introduction

Regardless of extensive development of commercial software for static and dynamic analysis of mechanical systems, there is still a need for more specific models and programs which can be used by small enterprises dealing with design and production of cranes. A firm's own models and programs, designed for special devices, are especially useful at the initial design phase [1]. Good numerical effectiveness and adaptation of the interface to customer needs results in the possibility of using the programs without the necessity of long training and specialist knowledge. The models and programs for static analysis of a lattice-boom crane presented in the paper are examples of such a project developed for Protea. The program enables the user to analyse lifting performance of the crane in several configurations. These are defined by means of a radius crane.

Lattice-boom cranes are often used when large and heavy items have to be lifted. Due to their structure cranes with lattice-booms are examples of slender structures for which analysis of stability [3, 5, 7] and buckling [8] is especially important. Thus, an efficient model for static analysis which incorporates all necessary parameters of the crane helps engineers at the design stage.

2. Crane model

Figure 1 presents a model of the crane under consideration. It is assumed that the main parts of the crane, such as the lattice-boom (K), mast (A) and rope systems (Z_w, G, B), are flexible. The inertial

* To whom correspondence should be addressed

coordinate system $\{x, y, z\}$ is placed at point O on the mast's axis of symmetry. Lateral tilt (heel) and trim are considered by means of gravity forces. The model is derived using homogenous transformations and the rigid finite element method for discretisation of the lattice-boom.

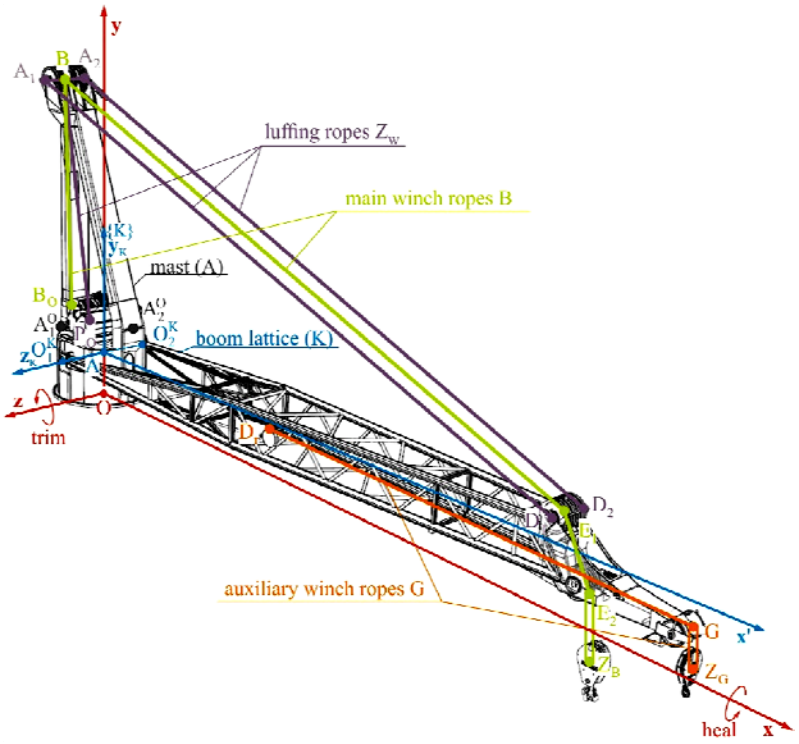

Fig.1. Crane model

The equilibrium equations of the crane are derived from the Lagrange equations in the following form

$$\frac{\partial V_s}{\partial q_k} + \frac{\partial V_g}{\partial q_k} = Q_k \tag{2.1}$$

where V_s is the energy of spring deformation of the system, V_g is the potential energy of gravity forces, Q_k are generalised forces resulting from external forces (loads and constraint reactions), q_k is k-th generalised coordinate.

Thus, generalised coordinates, energy of spring deformation for flexible components and generalised forces for parts of the crane have to be defined.

2.1. Lattice-boom

It is assumed that the main structure of the lattice-boom consists of boom sections connected consecutively. The boom section in general can be treated as a spatial truss (Fig.2a) with a different number of members connecting the four main beams, which can also differ in mass and geometry parameters.

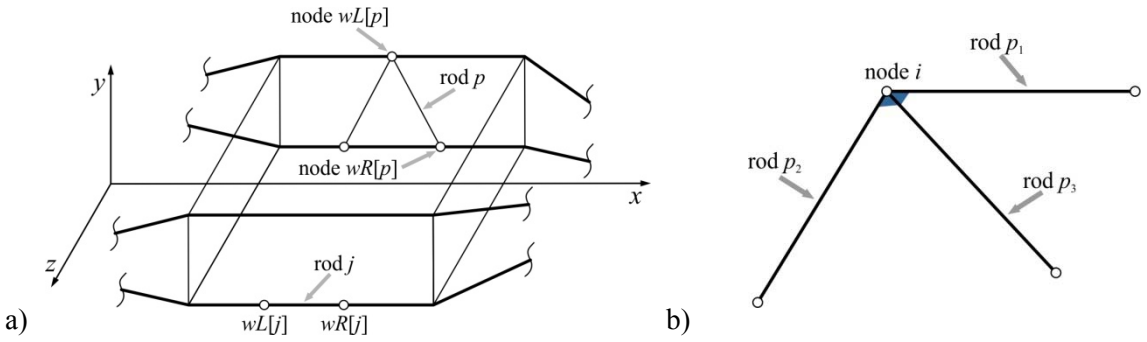

Fig.2. Beam model of a lattice-boom a) boom segment, b) node with rods

The members of the truss section are treated as beams, which means that they undergo bending, shearing as well as longitudinal and torsional deformations. The rods (members of the truss section) are firmly connected in a node (Fig.2b), which means that the displacements of the rods in node i ($i = 1 \ldots n$) are the same. In order to model the boom segment, it is important to define the nodes which are at the end of the rod members. The initial position of all nodes before deformation of the lattice-boom is known in the following form

$$\boldsymbol{r}_i^0 = \begin{bmatrix} x_i^0 \\ y_i^0 \\ z_i^0 \end{bmatrix} \qquad \text{for} \quad i = 1 \ldots n . \tag{2.2}$$

The coordinates of vectors (2) are defined in the global reference. The position and configuration of each rod of the boom ($p = 1 \ldots m$) are defined by its left $wL[p]$ and right nodes $wR[p]$. The orientation of the rods is defined using ZYX Euler angles and the geometry of the boom is described by means of homogenous transformations. The vector of generalised coordinates describing the displacements of the nodes consists of six components

$$\boldsymbol{q}_i = \begin{bmatrix} x_i & y_i & z_i & \varphi_i & \theta_i & \psi_i \end{bmatrix}^T = \left(q_{i,j} \right)_{\substack{i=1,\ldots,n \\ j=1,\ldots,6}} \tag{2.3}$$

where x_i, y_i, z_i are translations in the x, y, z directions respectively in the global coordinate system, $\varphi_i, \theta_i, \psi_i$ are the respective ZYX Euler angles.

It is assumed that axes of the local coordinate system $\{\}^{\sim}$ of the node are parallel to the global coordinate system $\{\}$. When coordinate systems are chosen in such a way, the transformation of coordinates from the local system of node $\{i\}^{\sim}$ to the global system $\{\}$ can be performed according to the formula

$$\boldsymbol{r}_i = \overline{\boldsymbol{r}}_i + \boldsymbol{R}_i \boldsymbol{r}_i' \tag{2.4}$$

where $\overline{\boldsymbol{r}}_i = \begin{bmatrix} x_i \\ y_i \\ z_i \end{bmatrix}$ is the vector of translational coordinates of the node, $\boldsymbol{R}_i = \boldsymbol{R}_i^{\psi} \boldsymbol{R}_i^{\theta} \boldsymbol{R}_i^{\varphi}$ is the rotation matrix,

$$\boldsymbol{R}_i^{\psi} = \begin{bmatrix} c\psi_i & -s\psi_i & 0 \\ -s\psi_i & c\psi_i & 0 \\ 0 & 0 & 1 \end{bmatrix}, \quad \boldsymbol{R}_i^{\theta} = \begin{bmatrix} c\theta_i & 0 & s\theta_i \\ 0 & 1 & 0 \\ -s\theta_i & 0 & c\theta_i \end{bmatrix}, \quad \boldsymbol{R}_i^{\varphi} = \begin{bmatrix} 1 & 0 & 0 \\ 0 & c\varphi_i & -s\varphi_i \\ 0 & s\varphi_i & c\varphi_i \end{bmatrix}, \quad c\alpha_i = \cos\alpha_i , \quad s\alpha_i = \sin\alpha_i ,$$

$\alpha_i \in \{\psi_i, \theta_i, \varphi_i\}$, $\boldsymbol{r}'_i$ is the coordinate vector in the local system $\{i\}^{\sim}$, $\boldsymbol{r}_i$ is coordinate vector in the global system $\{\}$.

Having used homogenous transformations, formula (2.4) takes the following form

$$\boldsymbol{r}_i = \begin{bmatrix} x_i & y_i & z_i & 1 \end{bmatrix}^T = \boldsymbol{B}_i \begin{bmatrix} x'_i & y'_i & z'_i & 1 \end{bmatrix}^T = \boldsymbol{B}_i \boldsymbol{r}'_i \tag{2.5}$$

where $\boldsymbol{B}_i = \begin{bmatrix} \boldsymbol{R}_i & \overline{\boldsymbol{r}_i} \\ 0 & 1 \end{bmatrix}$.

Rod elements are discretised using the rigid finite element method [6] and respective forces and moments transferred by spring damping elements (sdes) (Fig.3) of the rods are calculated [2, 4].

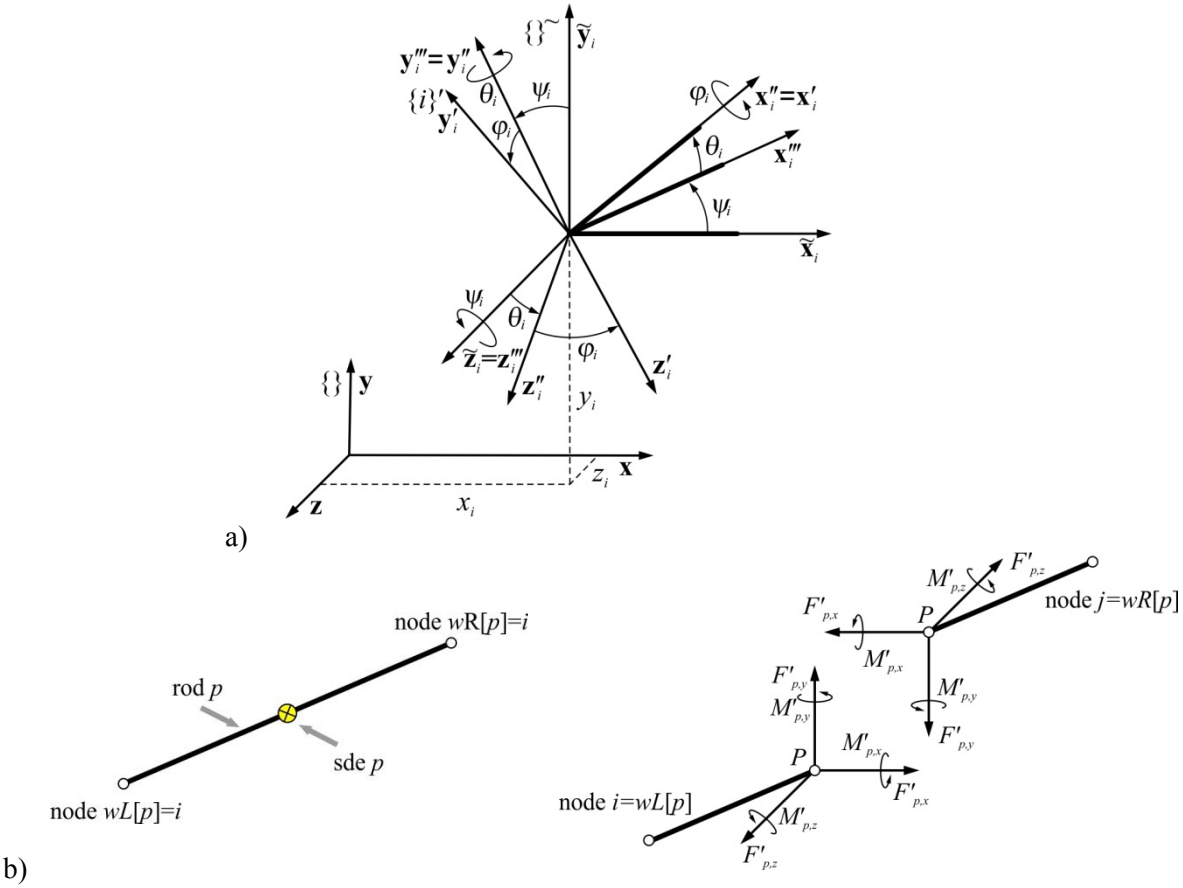

Fig.3. Nodes and rods a) generalised coordinates of nodes, b) discretization of rod p.

Forces $\boldsymbol{F}'_p = \begin{bmatrix} F'_{p,x} & F'_{p,y} & F'_{p,z} \end{bmatrix}^T$ and moments $\boldsymbol{M}'_p = \begin{bmatrix} M'_{p,x} & M'_{p,y} & M'_{p,z} \end{bmatrix}^T$ transferred by spring-damping elements are derived [3] and introduced into the equilibrium equations by means of generalized forces [5] at the end nodes of rod p.

Each rod is loaded with a force induced by gravity forces

$$\boldsymbol{F}_p^{(g)} = gm_p \begin{bmatrix} \alpha_H \\ -1 \\ -\alpha_T \end{bmatrix} \tag{2.6}$$

where g is gravity accelertion, α_T is the trim angle, α_H is the heel angle.

This force is distributed to the left and right part of the rod.

2.2. Mast

It is assumed that the mast is an A-frame with two segments (Fig.4). The mast is discretized in the same way as the boom by dividing the segments into nodes and rods.

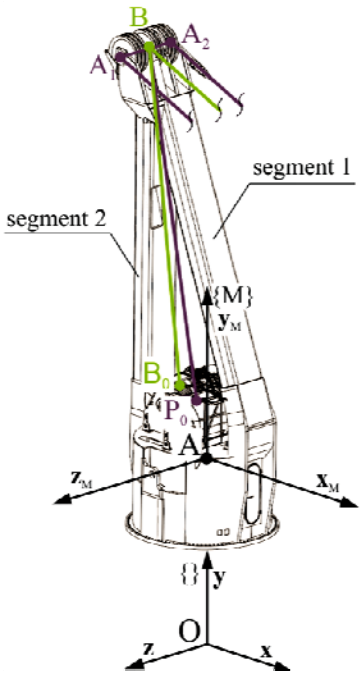

Fig.4. A-frame model of the mast.

2.3. Rope systems

Three rope systems which connect winches, column, and boom with a load are modelled (Fig.1): luffing mechanism (Z_w), main lifting system (B) and auxiliary lifting mechanism (G).

All three models are obtained in a similar way by adding derivatives of spring deformation energy of the ropes to the equilibrium equations. Considerations concerning the energy of rope deformation are presented below.

Figure 5 presents all three rope systems.

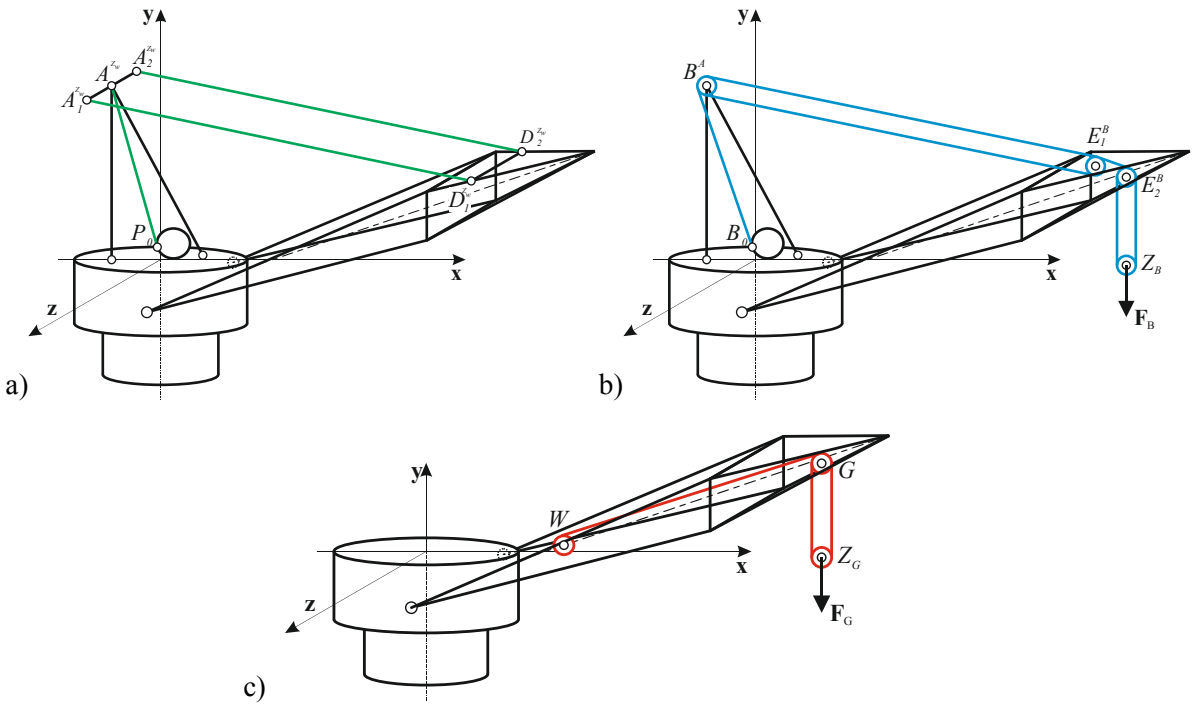

Fig.5. Rope systems: a) luffing mechanism, b) main lifting system, c) auxiliary lifting system.

Potential energy of rope deformation (Fig.6) can be calculated as follows

$$V_{Zw} = \frac{1}{2} c_{Zw} \Delta_{Zw}^2 , \tag{2.7a}$$

$$V_B = \frac{1}{2} c_B \Delta_B^2 , \tag{2.7b}$$

$$V_G = \frac{1}{2} c_G \Delta_G^2 \tag{2.7c}$$

where: $\Delta_{Zw} = L_{Zw} - L_{Zw}^0$, $\Delta_B = L_B - L_B^0$, $\Delta_G = L_G - L_G^0$, L_{Zw}^0, L_B^0, L_G^0 are the lengths of respective ropes before deformation of the system, c_{Zw}, c_B, c_G are stiffness coefficients of ropes, L_{Zw}, L_B, L_G are the lengths of ropes after loading.

The length of the rope after loading L_{Zw}, L_B, L_G depends on the coordinates of points through which the rope passes and on the transmission ratio in the section considered.

Let us consider a general case, in which the potential energy of rope deformation is written in the form

$$V_l = \frac{1}{2} c_l \Delta_l^2 \tag{2.8}$$

where: c_l is the stiffness coefficient of the rope, $\Delta_l = L - L_0$ is the elongation of the rope, L_0 is the initial length of the rope, L is the final length of the rope.

It is also assumed that

$$L = \sum_{j=1}^{k} i_j d_j , \tag{2.9}$$

where i_j is the transmission of the rope in section j connecting points N and M, d_j is the distance between points N and M.

When local coordinates of points N and M are defined by vectors $\boldsymbol{r}'_N$, $\boldsymbol{r}'_M$ then their coordinates in the global coordinate system can be calculated as follows

$$\boldsymbol{r}_N = \boldsymbol{B}_N \boldsymbol{r}'_N, \tag{2.10a}$$

$$\boldsymbol{r}_M = \boldsymbol{B}_M \boldsymbol{r}'_M \tag{2.10b}$$

where $\boldsymbol{B}_N = \boldsymbol{B}_N(\boldsymbol{q}_N)$, $\boldsymbol{B}_M = \boldsymbol{B}_M(\boldsymbol{q}_M)$ are homogenous transformation matrices.

The distance d_j between points N and M can be calculated according to the following formula

$$d_j^2 = (\boldsymbol{r}_M - \boldsymbol{r}_N)^T (\boldsymbol{r}_M - \boldsymbol{r}_N). \tag{2.11}$$

Derivatives of energy (1) with respect to $\boldsymbol{q}_N$ and $\boldsymbol{q}_M$ take the form

$$\frac{\partial V}{\partial \boldsymbol{q}_{N,k}} = c_L \Delta_L \frac{\partial \Delta_L}{\partial \boldsymbol{q}_{N,k}} = -c_L \Delta_L i_L \frac{1}{d_j} \left(\boldsymbol{B}_{N,K} \boldsymbol{r}'_N\right)^T (\boldsymbol{r}_M - \boldsymbol{r}_N), \tag{2.12a}$$

$$\frac{\partial V}{\partial \boldsymbol{q}_{M,k}} = c_L \Delta_L \frac{\partial \Delta_L}{\partial \boldsymbol{q}_{M,k}} = -c_L \Delta_L i_L \frac{1}{d_j} \left(\boldsymbol{B}_{M,K} \boldsymbol{r}'_M\right)^T (\boldsymbol{r}_M - \boldsymbol{r}_N), \tag{2.12b}$$

for $k = 1,\ldots,6$.

Energy derivatives V_{Zw}, V_B, V_G are calculated according to the above formulae.

3. Validation

Equilibrium equations derived from (1) are written in the form of nonlinear algebraic equations as follows

$$\boldsymbol{F}(\boldsymbol{q}) = 0 \tag{3.1}$$

where $\boldsymbol{q}$ is the vector of generalised coordinates of the crane.

The iterative Newton method has been used in order to solve Eq.(3.1). In order to determine the gradient matrix, five-point finite differences have been used.

The model of the crane presented in Fig.1 consists of three segments: the boom is considered as segment *0* while segments *1* and *2* are parts of the mast.

In order to validate the model and subsequent programme, numerical simulations have been carried out and the results obtained have been compared with those from the ROBOT commercial software package based on the finite element method. The comparison is concerned with forces and stresses in chosen rods. The rigid finite element method enables calculations of forces and stresses in the middle of rods, while the finite element method gives results at the ends of rods, and thus some approximation had to be applied.

Comparisons have been carried out for the model of the crane presented in Fig.6. A simplified model of the connection between the crane and the base as well as between the column and the boom is used. It is assumed that forces $F_x = 40 \cdot 10^4$ N, $F_y = -$SWL, $F_z = -40 \cdot 10^4$ N act at point E_2 at the end of the boom.

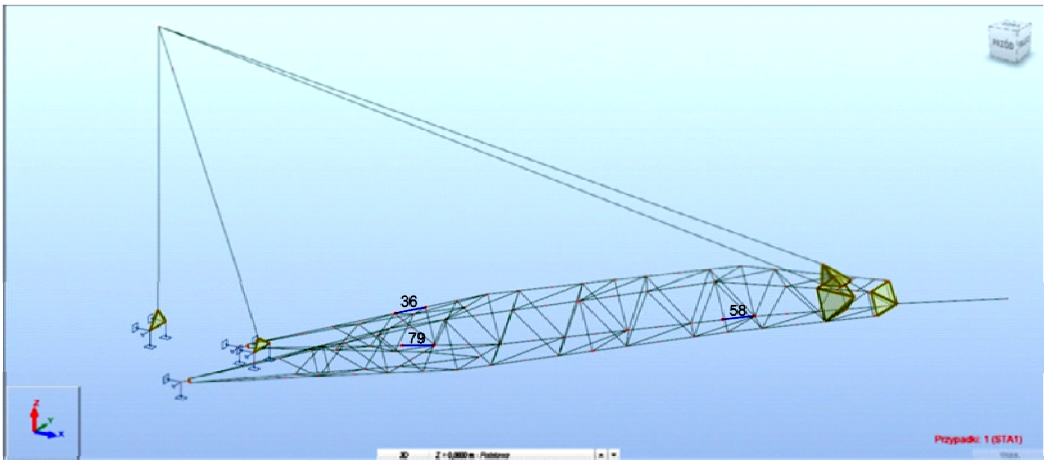

Fig.6. Model of the crane (ROBOT)

The influence of base inclination due to both heel and trim angles, of the deviation of the load (offlead and sidelead) and of the accelerations caused by waves, wind and gravity forces is taken into account.

Numerical simulations have been carried out for the crane from Fig.1 for crane radius $R = 2.7$ m(SWL = 268 mT), $R = 17$ m(SWL = 460 mT) and $R = 30$ m(SWL = 460 mT). Table 1 presents the deflections of the boom (point G) obtained using the authors' program and ROBOT software. Total deflections differ by less than 3%.

Table 1. Deflections of the boom at point G.

Crane radius [m]	**Authors' program**					**ROBOT**					**Difference %**
	SWL [mT]	u_x [m]	u_y [m]	u_z [m]	u [m]	SWL [mT]	u_x [m]	u_y [m]	u_z [m]	u [m]	
2.7	*268*	*77.99*	*-10.12*	*-10.59*	*79.4*	*268*	*78.0*	*-9.2*	*-11.0*	*79.3*	*0.06*
17	*460*	*59.64*	*-43.30*	*-10.00*	*74.4*	*460*	*58.5*	*-41.8*	*-11.0*	*72.7*	*2.21*
30	*460*	*16.18*	*-70.67*	*-5.69*	*72.7*	*460*	*16.6*	*-69.7*	*-6.6*	*72.0*	*1.06*

Comparison of forces in the rope systems is presented in Tab.2.

Table 2. Forces in the rope systems.

Crane radius [m]	**Authors' program**		**ROBOT**		**Difference %**	
	Luffing Z_w [kN]	Main B [kN]	Luffing Z_w [kN]	Main B [kN]	Luffing Z_w	Main B
2.7	*798*	*755*	*803*	*752*	*0.57*	*-0.41*
17	*1019*	*754*	*1003*	*752*	*-1.57*	*-0.32*
30	*870*	*427*	*858*	*425*	*-1.34*	*-0.51*

Table 3 presents comparison of forces and stresses for crane radius $R = 30$ m, in three rods shown in Fig.6.

Table 3. Forces and stress in rods.

Rod number	**Authors' program**		**ROBOT**		**Difference %**	
	F_x [kN]	$\frac{\sigma_{max}+\sigma_{min}}{2}$ [MPa]	F_x [kN]	$\frac{\sigma_{max}+\sigma_{min}}{2}$ [MPa]	F_x [kN]	$\frac{\sigma_{max}+\sigma_{min}}{2}$ [MPa]
36	*2292*	*159*	*2275*	*160*	*0.7*	*0.5*
79	*276*	*-89*	*280*	*91*	*1.16*	*2.14*
58	*2590*	*142*	*2574*	*144*	*0.63*	*0.91*

It is important to note that the compatibility of results is satisfactory despite the differences in models. For example, in the authors' model the flexibility of the base is not taken into account unlike in the ROBOT model; the model presented takes into consideration flexibility and the transmission ratio while in ROBOT the rope systems are modelled as beams.

4. Final remarks

In the paper, a model of a lattice-boom crane is presented. It is assumed that the column, boom and rope systems are flexible. The rigid finite element method is used to discretize the column and the lattice-boom crane. In many applications the rigid finite element method has been used to discretize beam-like links and plates. This new approach for modelling truss structures proves that the method can be used even for broader applications. The model and program developed have been validated by comparison of the authors' own results with those obtained from commercial software. Good compatibility of results has been achieved and this enables further research in dynamics of such cranes to be undertaken.

References

[1] Adamiec-Wójcik I., Fałat P., Maczyński A. and Wojciech S. 2009): *Load stabilisation an a-frame - a type of an offshore crane.* – Archive of Mechanical Engineering, vol.56, No.1, pp.37-59.

[2] Drąg Ł. (2017): *Modelling of lines, risers and cranes by means of the rigid finite element method*. – Bielsko-Biała: University of Bielsko-Biała Press.

[3] Kong X., Qi Z. and Wang G. (2015): *Elastic instability analysis for slender lattice-boom structures of crawler cranes*. – Journal of Constructional Steel Research, vol.115, pp.206-222.

[4] Nowak P., Nowak A. and Metelski M. (2017): *Modelling of vibration and large deflections of lattice-boom structures of cranes by means of rigid finite element method*. – In Conference Proceedings of DSTA 2017: Mathematical and numerical aspects of dynamical system analysis (eds. J. Awrajcewicz et al.) Łódź, 2017, pp.425-436.

[5] Wang G., Qi Z. and Kong X. (2015): *Geometrical nonlinear and stability analysis for slender frame structures of crawler cranes*. – Engineering Structures, vol.83, pp.209-222.

[6] Wittbrodt E., Adamiec-Wójcik I. and Wojciech S. (2006): *Dynamics of flexible multibody systems – rigid finite element method*. – Berlin: Springer.

[7] Sun X. (2002): *Design of unconventional slender steel structures by stability analysis*. http:/hdl.handle.net/10397/3454.

[8] Yao J., Qiu X., Zhou Z., Fuc Y., Xinga F. and Zhao E. (2015): *Buckling failure analysis of all-terrain crane telescopic boom section*. – Engineering Failure Analysis, vol.57, pp.105–117.

Received: June 25, 2018

Revised: July 3, 2018